Sesquiterpenes from *Oplopanax horridus*

Taichi Inui,[†,‡,⊥] Yuehong Wang,[‡] Dejan Nikolic,[†] David C. Smith,[§] Scott G. Franzblau,[‡] and Guido F. Pauli*[,†,‡]

Department of Medicinal Chemistry and Pharmacognosy and Institute for Tuberculosis Research, College of Pharmacy, University of Illinois at Chicago, Chicago, Illinois 60612, and Alaska Green Gold, Anchorage, Alaska 99510

Received October 21, 2009

From the anti-TB active fractions of the inner stem bark of *Oplopanax horridus,* two new heterocyclic nerolidol derivatives, 3,10-epoxy-3,7,11-trimethyldodeca-1,6-dien-11-ol, named neroplomacrol (**1**), and *rel*-(3*S*,6*R*,7*S*,10*R*)-7,10-epoxy-3,7,11-trimethyldodec-1-ene-3,6,11-triol, named neroplofurol (**2**), were isolated together with oplopandiol (**3**), falcarindiol (**4**), and sesamin (**5**). Extensive spectroscopic analysis revealed that **1** possesses a novel 3,10-oxanonacyclic ring system. Computer-iterated full spin system analysis led to the generation of ^{1}H NMR fingerprints that will facilitate future dereplication of analogues by providing characteristic spin−spin coupling patterns. The full spin analysis of **5** revealed asymmetric coupling patterns among the chemically equivalent spins, thus confirming the magnetic asymmetry of **5**. It was further demonstrated that ^{1}H NMR fingerprints and MS data enable dereplication of isolates at a submilligram levels including their relative configuration. Countercurrent concentration of the anti-TB activity of the ethnobotanical *O. horridus* versus the *Mycobacterium tuberculosis* Erdman strain led to polyynes **3** and **4** as main anti-TB active principles. Their synergistic behavior is linked to a complex fraction containing the new nerolidiol sesquiterpenes, **1** and **2**, as phytochemical marker compounds.

Oplopanax horridus (Sm.) Miq. (Araliaceae) (syn. *Fatsia horrida* (Sm.) Benth. & Hook.; *Echinopanax horridus* (Sm.) Decne. & Planch; *Panax horridum* (Sm.)), commonly known as devil's club, is an abundant deciduous shrub found along the Northern Pacific coast of North America. It is one of the most important plants among native tribes in the Alaskan region due to the fact that it has been used extensively in shamanistic rituals, as well as a treatment for various ailments, including tuberculosis.[1−3] There is a consistency in the applications of *O. horridus* as a medicinal plant even among tribes too far apart for direct communication, and at least eight distinctive cultural groups use *O. horridus* bark for tuberculosis treatment.[4] The crude extract of *O. horridus* was found to be active against *Mycobacterium tuberculosis* Erdman and *M. avium* by disk diffusion assay.[5]

Two independent GC-MS analyses of *O. horridus* identified 36 sesquiterpenes and oxygenated sesquiterpenes, including *trans*-nerolidol.[6,7] So far, the structures of five polyynes have been reported from the inner stem bark of the plant.[8] The absolute configuration of oplopandiol acetate, one of the five reported polyynes, has been determined as (11*S*, 16*S*) by the modified Mosher method and was confirmed by total synthesis.[9] The five polyynes from the inner stem bark have shown moderate antimycobacterial activities among the known constituents of *O. horridus*.[8,10] Recent investigations involving absorption-free countercurrent chromatography have proven the presence of anti-TB synergistic interactions among fractions of *O. horridus*.[11] When synergy is present, chemical standardization of ethnobotanical preparations requires marker compounds for the active extracts/fractions regardless of the activities of markers as individual compounds.

Dereplication, i.e., the process of rapid identification of already known natural products, can facilitate the standardization of ethnobotanicals with synergistic activity, as structurally similar secondary metabolites often have similar but distinct spectroscopic properties. Even subtle differences in the ^{1}H spin systems of two structures can give rise to second- or higher-order spin−spin coupling effects, which often produce significant differences in the splitting patterns of the ^{1}H NMR signals. Hence, a computer-iterated full spin system analysis of the isolated compounds will serve to facilitate the process of dereplication by providing more accurate spectral interpretation as well as characteristic ^{1}H NMR fingerprints for later comparison. Not only are observed complex peak patterns unique for each compound, they can also be fully reproduced by spectral simulation from the tabulated spin system parameters even if future spectra are measured at different magnetic field strengths. Therefore, a complete ^{1}H NMR spectral analysis facilitates unambiguous, yet rapid structure dereplication through comparison of NMR fingerprints and represents complex but unique splitting patterns that are present in the majority of the high-resolution ^{1}H signals.[12,13]

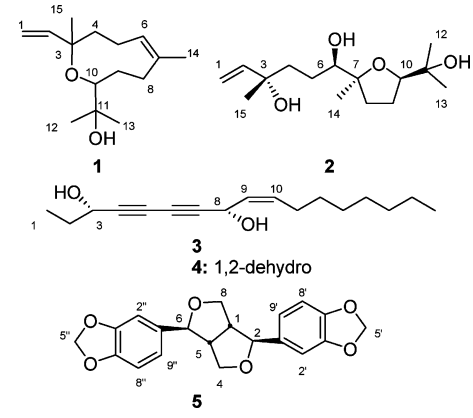

Results and Discussion

The inner stem bark of *O. horridus* was consecutively extracted with CH_2Cl_2, MeOH, and 50% aqueous MeOH. In order to remove the anti-TB inactive lipophilic and hydrophilic constituents, the combined extracts were partitioned between *n*-hexane−EtOAc−MeOH−water (HEMWat) solvent systems (SSs), first HEMWat −8 then HEMWat 0, respectively.[14] The anti-TB activity was concentrated in the upper phase of HEMWat 0, which was further separated by countercurrent chromatography (CCC) involving a sequence of finely tuned two-phase SSs, i.e., gradient-array CCC.[15] Further MPLC separation of the two most active fractions

* To whom correspondence should be addressed. Tel: 312-355-1949. Fax: 312-996-2693. E-mail: gfp@uic.edu.
† Department of Medicinal Chemistry and Pharmacognosy, College of Pharmacy, University of Illinois at Chicago.
‡ Institute for Tuberculosis Research, College of Pharmacy, University of Illinois at Chicago.
§ Alaska Green Gold, Anchorage, Alaska.
⊥ Current address: Wm. Wrigley Jr. Company, Chicago, Illinois 60642.

10.1021/np900674d
Published on Web 03/10/2010

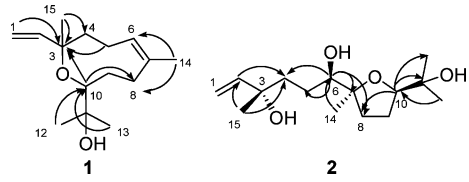

Figure 1. Key HMBC correlations of **1** and **2**.

led to the isolation of 3,10-epoxy-3,7,11-trimethyldodeca-1,6-dien-11-ol, named neroplomacrol (**1**), *rel*-(3*S*,6*R*,7*S*,10*R*)-7,10-epoxy-3,7,11-trimethyldodec-1-ene-3,6,11-triol, named neroplofurol (**2**), oplopandiol (**3**), falcarindiol (**4**), and sesamin (**5**).

In addition to being a gentle, loss-free, and linear scale-up method, the liquid−liquid nature of CCC proved to be advantageous for the initial fractionation of bioactive extracts due to the resolution characteristics of CCC SSs. The *K*-range of optimum resolution (B-region, typically $0.3 > K > 3.0$) is flanked by regions with reduced resolution and high retention (A- and C-regions, respectively), the latter of which became accessible only recently with the introduction of the EECCC and ReS methods.[14,16−18] In the present study, CCC's very limited capability of applying gradients was overcome by the gradient-array method, which applies several separation steps with SSs of graded polarity from the same SS family.[19,20] For example, reprocessing of the HEMWat 0 A-region fraction with the less polar HEMWat −2 SS started the gradient array by extending the CCC high-resolution window toward the former A-region and shifting the B-range to more lipophilic compounds. Bioassay-guided fractionation used the virulent Erdman strain of *M. tuberculosis* to prioritize subsequent MPLC separations, which led to isolation of **1**−**5**.

The ^{1}H NMR spectrum of **1** indicated the presence of two double bonds and four methyl groups. Three doublets of doublets at δ 5.899 (1H), 5.182 (1H), and 5.014 (1H) showed a coupling pattern characteristic of a terminal vinyl group having a small geminal coupling ($J = 1.7$ Hz), a *trans* vicinal coupling ($J = 17.4$ Hz), and a *cis* vicinal coupling ($J = 10.8$ Hz). One doublet appearing at δ 1.609 ($J = 1.3$ Hz) was consistent with a methyl group and suggested the presence of a methyl-substituted olefinic moiety with only allylic coupling. The ^{13}C NMR experiments, including DEPT-135 analysis, revealed that compound **1** contains 15 carbons, including five methylene carbons. One of the methylene carbons (sp^2-hybrized) appeared at δ 111.98 and confirmed the presence of a terminal vinyl moiety. HRESIMS revealed the molecular ion $[M + H]^+$ as 239.2013, possessing a molecular formula of $C_{15}H_{26}O_2$. Taking into consideration the double-bond equivalency derived from the indicated molecular formula, the presence of a single ring system was inferred. From the ^{13}C NMR spectrum, which indicated the presence of three heterosubstituted carbons, most likely oxygen, the ring system was alleged to contain an ether linkage. Extensive 2D NMR experiments led to the structural assignment of **1** as being an oxygenated sesquiterpene, formally derived from nerolidol, with a novel nine-membered macro-heterocyclic skeleton. An ether linkage between C-3 and C-10 was confirmed by the presence of HMBC cross-peaks from H-10 to C-3 (Figure 1). The spectroscopic data for **1** are consistent with the structure of 3,10-epoxy-3,7,11-trimethyldodeca-1,6-dien-11-ol. In line with its key structural features, the name neroplomacrol is proposed for **1**.

The ^{1}H NMR spectrum of **2** also indicated the presence of a terminal vinyl group, two oxygenated methines, and four methyl groups. The ^{13}C NMR spectrum showed a total of 15 carbon resonances including five heterosubstituted (oxygenated) carbons. DEPT-135 analysis revealed the presence of five methylene carbons, including one (sp^2-hybridized) appearing at δ 111.8 and assigned to the terminal carbon of a vinyl group. The presence of a saturated furan ring was suggested by ^{13}C resonances observed at δ 86.3 and 84.3 and a dd coupling pattern of the ^{1}H signal at δ 3.792 with coupling constants of 7.56 and 7.25 Hz. At this point, all of the data would also be consistent with an alternative structure containing a O-3/O-6 endoperoxide ring system corresponding to a molecular formula of $C_{15}H_{26}O_4$.[21] As such, a partial structure could not be directly verified by heteronuclear 2D NMR due to the disruption of the ^{1}H−^{13}C coupling pathways and only indirectly recognized by complete ^{1}H NMR spin analysis. Important evidence came from HRESIMS, which revealed a molecular ion at 295.1896 *m*/*z* consistent with a molecular formula of $C_{15}H_{28}O_4Na$. A D_2O exchange experiment resulted in a MS peak at 298 *m*/*z* (three mass units higher), which confirms the presence of three free OH groups in the molecule. Taken together, the spectroscopic data for **2** were consistent with the structure *rel*-(3*S*,6*R*,7*S*,10*R*)-7,10-epoxy-3,7,11-trimethyldodec-1-ene-3,6,11-triol (Figure 1). The carbon numbering scheme was selected in accordance with previous reports on this general compound class.[22] In line with the base structure of a tetrahydrofuran moiety, the name neroplofurol is proposed for **2**.

While this represents the first report of **2** being isolated from a natural source, its structure has previously been reported as a product of the biotransformation of *trans*-nerolidol with *Diplodia gossypina* ATCC 10936.[22] Although no ^{1}H NMR data were reported in this study, the authors kindly shared original NMR data of a series of in part unpublished sesquiterpenes that served as references in their assignment of the relative configurations of **2**.[23] Comparison of the ^{13}C NMR data of **2** with those of two previously identified isomers (Table 3) demonstrated a generally good match between **2** and the 3*S*,6*R*,7*S*,10*R*-isomer, whereas a 3.3 ppm chemical shift difference was noted for C-10 when compared with the 3*S*,6*S*,7*R*,10*R*-isomer. While the partial open-chain structure of **2** would require an X-ray diffraction analysis for full elucidation of its absolute configuration, NOE evidence (correlation between H-6 and Me-14) together with the results of molecular modeling provides support for the indicated relative configurational assignments of the tetrahydrofuran portion as well as the C-6 stereocenter in **2** (Figure 2).

In order to provide a point of reference for future dereplication of congeneric sesquiterpenes, a full spin system analysis of **2** was performed by means of iterative simulation using PERCH software (Table 2). While the observed coupling constant and chemical shift information is listed in the Experimental Section, the simulated spectra exhibited excellent agreement with the observed spectra for all spectral lines and line intensities. The characteristic ^{1}H NMR fingerprint of **2** is illustrated in Figure S1, Supporting Information.

Structures of **3** and **4** were identified by NMR and MS spectrometry and compared with the literature.[8,24] The ^{1}H NMR spectrum for **5** showed nine resonances, all of which appeared at shifts > 3.0 ppm. A signal at δ 5.29 (2H) suggested the presence of a methylene dioxide moiety, while the resonances at δ 6.880, 6.843, and 6.779 exhibited the characteristic ABX coupling pattern associated with a 1,2,4-trisubstituted aromatic ring system. EIMS analysis revealed a molecular ion at *m*/*z* 354. A database search based on the MS fragmentation pattern suggested that compound **5** was sesamin ($C_{20}H_{18}O_6$). Although a side-by-side comparison of the ^{1}H chemical shifts between **5** and the literature values of sesamin showed a reasonable match, an unambiguous dereplication of the isolate was complicated by the lack of information on the magnitude of coupling constants, especially for the signals at δ 3.088 and 4.222.[25−27] This gap most likely results from the complexity of spin systems that is characterized by the magnetic inequivalence of an otherwise symmetric dimeric molecule. The asymmetry in the *J* coupling pattern is apparent from the structure, in which two protons with identical chemical shifts (chemical equivalence) couple to the same proton, but with different *J*'s (magnetic inequivalence). For example, while H-2 and H-6 have the same chemical shift, and while both are coupled with H-1, the coupling constants $^3J_{1/2}$ and $^4J_{1/6}$ possess different values, resulting from different coupling pathways. Coupling asymmetry makes the spin system present in the ^{1}H spectrum of **5** a highly complex one. Hence, in order to

Table 1. NMR Data of **1** (400/100 MHz, $CDCl_3$)

pos.	δ_C, mult	δ_H mult (J in Hz)	HMBC	COSY
1	111.98, CH_2	5.182, dd (−17.4, 1.7)	2, 3	2
		5.014, dd (10.8, 1.7)	2, 3	2
2	146.28, CH	5.899, dd (−17.4, 10.8)	3, 4, 15	1a, 1b
3	73.73, qC			
4	43.39, CH_2	1.510, ddt (6.7, 2.2, 10.1)	3, 5, 6, 15	5
5	23.66, CH_2	2.023, m	3, 4	4, 6
6	125.77, CH	5.184, ddt (2.6, 1.3, 7.2)	4, 5, 7, 8, 14	5, 14
7	135.96, qC			
8	37.83, CH_2	2.233, m	6, 7, 9, 14	8b, 9a, 9b
		2.023, m	6, 9, 14	8a, 9a, 9b
9	30.71, CH_2	1.698, dddd (−13.7, 9.7, 7.0, 1.8)	7, 8	8a, 8b, 9b, 10
		1.336, dddd (−13.7, 10.6, 9.7, 4.8)	7, 8	8a, 8b, 9a, 10
10	78.93, CH	3.222, dd (10.6, 1.8)	3, 8, 9, 11, 12, 13	9a, 9b
11	73.90, qC			
12	25.64, CH_3	1.149, s	10, 11, 13	
13	24.97, CH_3	1.117, s	10, 11, 12	
14	16.10, CH_3	1.609, d (1.3)	6, 7	6
15	27.59, CH_3	1.242, s	2, 3, 4	

Table 2. NMR Data of **2** (400/100 MHz, $CDCl_3$)

pos.	δ_C, mult	δ_H, mult. (J in Hz)	HMBC	COSY
1	111.8, CH_2	5.211, dd (−17.31, −1.47)	2, 3	1a, 2
		5.048, dd (10.73, −1.47)	3	1b, 2
2	144.9, CH	5.842, dd (−17.31, 10.73)	3, 4, 15	1a, 1b,
3	72.8, qC			
4	39.2, CH_2	1.791, ddd (−14.30, 7.18, 7.08)	2, 3, 5, 6, 15	4b, 5a, 5b
		1.665, ddd (−14.30, 7.04, 6.97)	2, 3, 5, 6, 15	4a, 5a, 5b
5	26.3, CH_2	1.537, dddd (−14.28, 7.18, 6.97, 2.06)	3, 4	5b, 6
		1.341 (−14.28, 10.66, 7.08, 7.04)	3, 4, 6	5a, 6
6	77.8, CH	3.534, dd (10.66, 2.06)	4, 5, 7, 8	5a, 5b
7	86.3, qC			
8	31.3, CH_2	2.092, ddd (−12.50, 9.58, 5.69)	6, 7, 9, 10, 14	8b, 9a, 9b
		1.479, ddd (−12.50, 8.80, 7.22)	6, 7, 9, 10, 14	8a
9	26.9, CH_2	1.906, dddd (−12.56, 9.58, 7.56, 7.22)	7, 8, 10, 11	8a, 8b, 10
		1.882, dddd (−12.56, 8.80, 7.25, 5.69)		8, 10
10	84.3, CH	3.792, dd (7.56, 7.25)	8, 11, 12	9a/b
11	71.9, qC			
12	27.6, CH_3	1.250, s	10, 11, 13	
13	25.5, CH_3	1.110, s	10, 11, 12	
14	23.8, CH_3	1.140, s	6, 7, 8	
15	28.8, CH_3	1.276, s	2, 3, 4	

make unambiguous assignments for confirmation of the structure, a full spin system analysis was performed. The results are summarized in Table S4 (Supporting Information) and served to verify the complex nature of the spin coupling system. The ^1H fingerprint signals of **5** are shown in Figure S2. Protons H-2 and H-6 are both represented by an apparent doublet that, upon full spin analysis, reveals its nature of a 7-fold coupled ddddddd. Representing the most highly coupled protons in the molecule, the six small couplings (−0.7 to +0.1 Hz) lead to (a) broadening of the main doublet lines of H-2/6 and (b) occurrence of a complex "side band" pattern in the signals of coupled protons. Thus, full spin analysis and matching of all observed lines (Figure S2) is necessary to deduce the underlying J coupling pattern and explain deviations from the apparent (first-order) signal multiplicity. All values for geminal couplings, allylic couplings, and one W coupling ($^4J_{2,5} = {}^4J_{1,6}$) were deduced from spectral iterations to be negative. Lorentz−Gaussian resolution enhancement helped to reveal the hidden splitting of the methylene dioxide signals of H-5′/5″, which led to confirmation of the overall magnetic asymmetry of the molecule. It should be pointed out that the iteration results were able to reproduce the minor lines in the spectra that arise due to higher-order spin coupling effects (Figure S2).

From a stereochemical perspective, there are 10 possible stereoisomers for **5** ($2^4 = 16$ minus 6 achiral forms); only six of them would satisfy the H-1/H-5 symmetry criteria. In order to fit the observed $^3J_{1,5} = 9.2$ as well as $^3J_{1,2}$ and $^3J_{5,6} = 5.5$ relationships, and in approximation of residual conformational averaging in the

Table 3. NMR Data of **2** and Two Known Diastereomers[a]

	2		3*S*,6*R*,7*S*,10*R*		3*S*,6*S*,7*R*,10*R*[22]	
pos.	δ_C	δ_H	δ_C	δ_H	δ_C	δ_H
1	111.8	5.211	112.0	5.24	111.6	5.21
		5.048		5.07		5.03
2	144.9	5.842	145.3	5.86	145.4	5.91
3	72.8		73.0		72.9	
4	39.2	1.791	39.5	1.85	39.2	NA
		1.665		1.68		NA
5	26.3	1.537	26.6	1.58	25.9	NA
		1.341		1.38		NA
6	77.8	3.534	77.9	3.56	77.1	3.52
7	86.3		86.5		86.2	
8	31.3	2.092	31.7	2.12	31.6	NA
		1.479		1.50		NA
9	26.9	1.906	27.0	1.92	26.7	NA
		1.882				
10	**84.3**	3.792	**84.6**	3.81	**87.7**	3.77
11	71.9		72.0		70.7	
12	27.6	1.250	27.6	1.27	27.5	1.26
13	25.5	1.110	25.6	1.13	23.9	1.13
14	23.8	1.140	23.7	1.15	23.9	1.20
15	28.8	1.267	28.8	1.20	27.9	1.29

[a] Ref 22 and unpublished data provided by Dr. Wolf-Rainer Abraham, Braunschweig, Germany. The ^{13}C chemical shifts of **2** are in good agreement with those of the 3*S*,6*R*,7*S*,10*R* diastereomer, whereas a marked $\Delta\delta$ of 3.3 ppm at C-10 distinguishes it from the 3*S*,6*S*,7*R*,10*R* form.

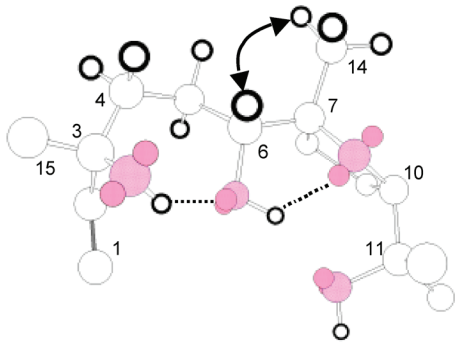

Figure 2. Observed NOE correlation between H-6 and Me-14 (arrow) and the coupling pattern in the tetrahydrofuran moiety (Table 2) of the average solution conformation of **2** were in agreement with results from MM2 force-field calculations. The framed circles represent the hydrogens, shaded circles represent the oxygens with lone electron pairs, and dashed lines indicate hydrogen bonds.

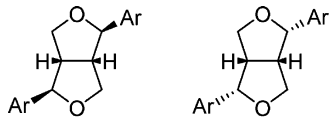

Figure 3. Relative configurations of **5** and epiasarinin (Ar = piperonyl moiety).

ring system, the orientations of H-1, H-2, and H5- had to satisfy two conditions: (a) φ(H-1−C-1−C-5−-5) ≈ 0° or 180° and (b) φ(H-1−C-1−C-2−H-2) ≈ ±30° or ±150°. If H-1 and H-5 were oriented *anti*, the dioxabicyclooctane ring would not have the flexibility to allow a conformation that would satisfy requirement (b). Conversely, if H-1 and H-5 were *syn* oriented, the two piperonyl moieties would also have to be *syn* in order to maintain overall symmetry. This leaves only two enantiomeric pairs, in contrast to the 10 possible stereoisomers for **5**, i.e., sesamin and epiasarinin (Figure 3).[28] Another important observation relates to significant shifts of line separations in the ^{1}H NMR signals of **5** due to higher-order spin coupling effects that are present. These effects produce complex additional weak intensity lines ("side bands"; Figure S2). For example, assuming a first-order analysis, the observed "visual *J* value", measured as a line distance between the two main lines of the H-2/6 signal, was 4.5 Hz. The iterated coupling constants $^3J_{1,2}$ and $^3J_{5,6}$ are 5.5 Hz. The "visual *J* value" is in good agreement with data reported for a compound whose configuration was confirmed by X-ray crystallography.[25] It remains important to realize that the interpretation of line separations under first-order assumptions can be misleading and deviate substantially from the real *J* values. In summary, the structure of **5** was, therefore, dereplicated as sesamin.

Compounds **1**−**5** were products of bioassay-guided fractionation, and antimycobacterial activities were determined only for the isolated compounds **1**−**4**, the exception being **5** due to insufficient quantities for testing. Compound **5** has previously been reported to be inactive (MIC >200 μg/mL) against *Mycobacteria tuberculosis* H37R*a* by microplate Alamar Blue assay (MABA).[29] The polyynes **3** and **4** were determined as active principles, showing MICs of 61.5 and 6.2 μg/mL, respectively. In contrast to previous reports, these polyynes were devoid of cytotoxicity against Vero cells and exhibited modest anti-TB selectivity with a selectivity index of 6.2 determined for **3**.[30] Although their isolation resulted from the CCC-concentrated active fraction, **1** and **2** did not exhibit significant anti-TB activities (MICs >128 μg/mL). Thus, **1** and **2** are new marker compounds for phytochemically complex anti-TB active fractions of *O. horridus*. This is in line with the previous report that established synergy among different chemical species as an important factor in the anti-TB activity of *O. horridus* and underscores the need to evaluate ethnobotanicals as complex mixtures rather than based on single active ingredients.[31]

Experimental Section

General Experimental Procedures. Optical rotation values $[\alpha]_D$ were measured on a Perkin-Elmer 241 polarimeter at 25 °C. UV λ_{max} values were determined with a Beckman DU 7000 UV/vis spectrometer. IR spectra were taken on a JASCO FT/IR-410 spectrometer. All ^{1}H NMR experiments were obtained at 400 or 900 MHz and performed on a Bruker AVANCE-400 spectrometer equipped with a 5 mm broadband ATM probe or AVANCE-900 spectrometer equipped with a 5 mm ^{1}H/^{13}C/^{15}N TCI probe, respectively, in 5 mm tubes using either $CDCl_3$ or CD_3OD as a solvent. All ^{13}C NMR experiments were obtained at 100 MHz and were performed on the Bruker AVANCE-400. The temperature was maintained at 25 °C. Chemical shifts (δ) are expressed in ppm with reference to the solvent signals (δ_H 7.240 and 3.300; δ_C 77.00 and 49.00, respectively). All NMR experiments were performed using standard Bruker pulse sequences. Spectral iterations for full ^{1}H NMR spin analysis were performed with the PERCH software package (ver. 2004a, PERCH Solutions, Kuopio, Finland). NMR processing used the NUTS software package (AcornNMR, Las Positas, CA), and line resolution of experimental data was enhanced by Lorentz−Gauss (LG) transformation using individually determined parameters. Molecular modeling was performed using Chem3D 7.0 (Cambridge Soft, Cambridge, MA). High-resolution mass spectra were obtained on a Micromass Q-Tof2 hybrid quadrupole/time-of-flight mass spectrometer equipped with electrospray ion source (ESI). Low-resolution mass spectra were obtained on a Varian 1200 quadrupole mass spectrometer in positive EI mode at −70 eV with scans of 50−650 *m/z*.

HSCCC separations were conducted on a CCC-1000 J-type three-coiled planetary motion HSCCC (Pharma-Tech Research Corp., Baltimore, MD) with 3 × 107 mL PTFE coils with 1.6 mm i.d., 2.6 mm o.d., and beta values from 0.47 to 0.73. FCPC separations were performed on a Kromaton FCPC instrument with a 200 mL rotor (Kromaton, Angers, France). Solvent system nomenclature is in accord with a previously published framework (GUESS).[14,17,18] Preparative MPLC was carried out using glass columns packed with various sorbents as follows: reversed-phase silica gel (LiChroprep RP-18), cyano-derivatized silica gel (CN, LiChroCN), or Sephadex LH-20. The MPLC system was equipped with a Waters Delta 600 multisolvent delivery system. HPLC was carried out with a Waters Delta 600 system equipped with a Waters 996 photodiode array (PDA) detector and YMC (ODS-AQ 20 × 250 mm) column. General fraction monitoring following preparative chromatographic separations was done by TLC analysis with precoated Alugram SIL G/UV plates (Macherey-Nagel, Düren, Germany) and by using *p*-anisaldehyde as detection reagent.

The anti-TB bioassay utilized was a MABA using the virulent *M. tuberculosis* Erdman strain (ATCC 35801).[32,33] Due to the relatively large number of fractions tested, percent inhibitions were determined at various concentrations for crude fractions. Rifampin was used as a positive control. Concurrent with the determination of MICs, samples were tested for cytotoxicity by determining the IC_{50} in Vero cells at concentrations less than or equal to 1% of the maximum achievable stock concentration in DMSO.[34] The anti-TB selectivity index was calculated as MIC/IC_{50}.

Plant Material. Inner stem bark of *O. horridus* from Alaska was harvested from wild cultures by one of the authors (D.C.S.) in 2002. Voucher specimens are deposited in the John G. Searle Herbarium at the Field Museum in Chicago, IL.

Extraction and Isolation. In order to extract the full range of constituents, three solvents of increasing polarity (dichloromethane, methanol, and 50% methanol in water) were used to exhaustively extract 157 g of powdered inner stem bark of *O. horridus* aided by an Ultra Turrax homogenizer. This yielded 12 g of total extract, which was further subject to solvent partitioning using the quaternary SS HEMWat −8 (*n*-hexane−EtOAc−MeOH−water, 8:2:8:2). The lower layer was separated, evaporated *in vacuo*, and subjected to a second partitioning step using the HEMWat 0 SS (*n*-hexane−EtOAc−MeOH−water, 5:5:5:5). The resulting upper layer was evaporated *in vacuo* to obtain 2.6 g of processed extract, which showed anti-TB activity (52% inhibition at 32 μg/mL). The other two layers were confirmed to be inactive.

The processed extract was subjected to gradient array CCC separation by means of FCPC, using the following sequence of SSs: HEMWat 0, HEMWat −2, HEMWat −4, and HEMWat −6 (S_F values: 67%, 68%, 72%, and 62%, respectively). Anti-TB evaluation of all subsequent fractions revealed the primary fractions F4−6 and 21−23 (defined by *K* values within the SSs used, see following paragraphs) to be the most active, showing 61% and 87% inhibition, respectively, at 32 μg/mL.

The combined primary fraction F4−6 (186.3 mg, $K = 1.64-2.12$ in HEMWat 0) was subjected to MPLC separation on RP-18 stationary phase. A linear MeCN−water gradient from 100% water to 50% water within 150 min and with a 5 mL/min flow rate was employed. Compound **1** eluted at t_R 34−38 min. The fractions were evaluated by TLC, where **1** (78.9 mg) appeared as a dark green spot upon chemical detection. The secondary fraction F3−13 (19.2 mg) was subject to preparative LH-20 isocratic MPLC separation with EtOAc as the mobile phase. Compound **2** eluted at t_R 590−630 min. The fractions were evaluated by TLC, where **2** (1.38 mg) appeared as a green spot upon chemical detection.

Combined primary fractions F21−23 (191.3 mg, $K = 0.97-2.48$ in HEMWat −4) was separated by HSCCC using a SS consisting of *n*-hexane−DCM−MeOH−water (7:3:6:4) with the upper (organic) as mobile phase and an S_F value of 64%. Compound **3** (20.4 mg) was eluted at $K = 1.33$. TLC analysis revealed **3** as a red spot upon anisaldehyde detection. A secondary HSCCC fraction with $K = 0.96-1.04$ in the DCM solvent system (21.2 mg) was further separated by MPLC using a cyano-derivatized stationary phase. A gradient from *n*-hexane to a 9:1 mixture of MeOH and *i*PrOH was employed, using a linear gradient from 97% to 94% *n*-hexane within 90 min at a flow rate of 2 mL/min. Compound **4** (2.9 mg) eluted at t_R 165 to 175 min. The fractions were evaluated by TLC, where **4** appeared as a dark red spot upon anisaldehyde detection. Another secondary HSCCC fraction with $K_D = 0.86-0.88$ (6.4 mg) was further purified by semipreparative RP-18 HPLC. A linear MeCN−water gradient was employed ranging from 45% to 20% water within 50 min at a flow rate of 3 mL/min. Fractions were collected manually on the basis of the PDA detector response. Compound **5** (0.38 mg) eluted at t_R between 19.1 and 21.8 min.

Neroplomacrol (1): colorless solid; mp 126−129 °C; $[\alpha]^{25}_D$ +17.3 (*c* 1.00, MeOH); UV (MeOH) λ_{max} (log ε) 230 (1.73) nm; IR (MeOH) λ_{max} 3390, 2936, 1386, 1167, 1087, 925 cm^{-1}; ^1H and ^{13}C NMR (CD_3OD 400 MHz) see Table 1; HRESIMS *m/z* 239.2013 (calcd for $C_{15}H_{27}O_2$, 239.2011, $\Delta = 0.2$ mamu).

Neroplofurol (2): colorless solid; mp 130−132 °C; $[\alpha]^{25}_D$ −23.7 (*c* 0.013, MeOH); UV (MeOH) λ_{max} (log ε) 224 (2.83) nm; IR (solid) λ_{max} 3433, 2985, 1309, 1089 cm^{-1}; ^1H and ^{13}C NMR (CD_3OD 400 MHz) see Table 2; HRESIMS *m/z* 295.1896 (calcd for $C_{15}H_{28}O_4Na$, 295.1885, $\Delta = 1.1$ mamu).

Oplopandiol (3): colorless solid; ^1H NMR ($CDCl_3$, 400 MHz) δ 5.589 (1H, ddt, $J = 10.7$, 0.8, 7.3 Hz, H-10), 5.492 (1H, ddt, $J = 10.7$, 8.2, 1.5 Hz, H-9), 5.180 (1H, d, $J = 8.2$ Hz, H-8), 4.362 (1H, dd, $J = 6.7$, 6.7 Hz, H-3), 2.082 (2H, ddt, $J = 7.3$, 1.5, 7.4 Hz, H-11), 1.734 (1H, ddq, $J = 11.9$, 6.7, 7.4 Hz, H-2a), 1.714 (1H, ddq, $J = 11.9$, 6.7, 7.4 Hz, H-2b), 1.360 (2H, dt, $J = 7.4$, 7.3 Hz, H-12), 1.260 (8H, m, H-13, H-14, H-15, H-16), 1.010 (3H, dd, $J = 7.4$, 7.4 Hz, H-1), 0.863 (3H, t, $J = 6.9$ Hz, H-17); ^{13}C NMR ($CDCl_3$, 100 MHz) δ 134.62 (CH, C-9), 127.71 (CH, C-10), 80.67 (C, C-4), 79.20 (C, C-7), 68.95 (C, C-6), 68.84 (C, C-5), 64.06 (CH, C-3), 58.06 (CH, C-8), 31.78 (CH_2, C-16), 30.61 (CH_2, C-2), 29.26 (CH_2, C-12), 29.14 (CH_2, C-13), 29.09 (CH_2, C-14), 27.67 (CH_2, C-11), 22.68 (CH_2, C-15), 14.08 (CH_3, C-17), 9.27 (CH_3, C-1); EIMS *m/z* 262 $[M]^+$ (15), 244 (55), 159 (50), 145 (60), 131 (62), 115 (95), 91 (100), 77 (62), 57 (97).

Falcarindiol (4): pale yellow solid; ^1H NMR ($CDCl_3$, 400 MHz) δ 5.927 (1H, dddd, $J = 17.3$, 10.1, 5.2, 0.3 Hz, H-2), 5.589 (1H, ddt, $J = 10.7$, 0.8, 7.3 Hz, H-10), 5.492 (1H, ddt, $J = 10.7$, 8.2, 1.5, 1.3 Hz, H-9), 5.452 (1H, dd, $J = 17.3$, 1.4 Hz, H-1a), 5.241 (1H, dd, $J = 10.1$, 1.4 Hz, H-1b), 5.180 (1H, dd, $J = 8.2$, 1.3 Hz, H-8), 4.920 (1H, brd, $J = 5.2$ Hz, H-3), 2.082 (2H, ddt, $J = 7.3$, 1.5, 7.4 Hz, H-11), 1.360 (2H, dt, $J = 7.4$, 7.3 Hz, H-12), 1.264 (8H, m, H-13, H-14, H-15, H-16), 0.860 (3H, t, $J = 6.9$, H-17); EIMS *m/z* 260 $[M]^+$ (10), 207 (21), 135 (42), 91 (49), 79 (52), 57 (100).

Sesamin (5): pale yellow solid; ^1H NMR ($CDCl_3$, 900 MHz) see S2 and S14 (Supporting Information).

Acknowledgment. We thank Drs. D. Lankin at UIC and M. Niemitz of PERCH Solutions Ltd., Kuopio (Finland), for spectroscopic support and very helpful discussions on various NMR topics, as well as help during manuscript preparation. We are much indebted to Dr. W.-R. Abraham, Braunschweig (Germany), for his diligence and open willingness to share NMR data, and are grateful to Drs. D. Doel Soejarto and A. Libman at UIC for their support in depositing the herbal specimen.

Supporting Information Available: ^1H, ^{13}C, ^1H,^1H−COSY, gHSQC, and gHMBC NMR spectra of **1** and **2** are available free of charge via the Internet at http://pubs.acs.org.

References and Notes

(1) McGregor, M. *Alaska Med.* **1981**, *23*, 65–69.
(2) Moerman, D. E. *Medicinal Plants of Native America*; University of Michigan Museum of Anthropology: Ann Arbor, MI, 1986; Vol. 2, pp 312−314.
(3) Smith, G. W. *J. Ethnopharmacol.* **1983**, *7*, 313–320.
(4) Turner, N. J. *J. Ethnobiol.* **1982**, *2*, 17–38.
(5) McCutcheon, A. R.; Stokes, R. W.; Thorson, L. M.; Ellis, S. M.; Hancock, R. E. W.; Towers, G. H. N. *Intl. J. Pharmacogn.* **1997**, *35*, 77–83.
(6) Bloxton, J. D.; Marderosian, A. D.; Gibbs, R. *Econ. Bot.* **2002**, *56*, 285–287.
(7) Garneau, F.-X.; Collin, G.; Gagnon, H.; Jean, F.-I.; Strobl, H.; Pichette, A. *Flavour Fragrance J.* **2006**, *21*, 792–794.
(8) Kobaisy, M.; Abramowski, Z.; Lermer, L.; Saxena, G.; Hancock, R. E. W.; Towers, G. H. N.; Doxsee, D.; Stokes, R. W. *J. Nat. Prod.* **1997**, *60*, 1210–1213.
(9) Xu, L.; Wu, X. H.; Zheng, G. R.; Cai, J. C. *Chin. Chem. Lett.* **2000**, *11*, 213–216.
(10) Deng, S.; Chen, S.-N.; Yao, P.; Nikolic, D.; van Breemen, R. B.; Bolton, J. L.; Fong, H. H. S.; Farnsworth, N. R.; Pauli, G. F. *J. Nat. Prod.* **2006**, *69*, 536–541.
(11) Inui, T.; Wang, Y.; Deng, S.; Smith, D. C.; Franzblau, S. G.; Pauli, G. F. *J. Chromatogr., A* **2007**, *1151*, 211–215.
(12) Niemitz, M.; Laatikainen, R.; Chen, S.-N.; Kleps, R.; Kozikowski, A. P.; Pauli, G. F. *Magn. Reson. Chem.* **2007**, *45*, 878–882.
(13) Jaki, B.; Franzblau, S.; Pauli, G. F. *Phytochem. Anal.* **2004**, *15*, 213–219.
(14) Friesen, J. B.; Pauli, G. F. *J. Liq. Chromatogr. Relat. Technol.* **2005**, *28*, 2777–2806.
(15) Case, R. J.; Wang, Y.; Franzblau, S. G.; Soejarto, D. D.; Matainaho, L.; Piskaut, P.; Pauli, G. F. *J. Chromatogr., A* **2007**, *1151*, 169–174.
(16) Berthod, A.; Friesen, J. B.; Inui, T.; Pauli, G. F. *Anal. Chem.* **2007**, *79*, 3371–3382.
(17) Friesen, J. B.; Pauli, G. F. *J. Chromatogr., A* **2009**, *1216*, 4225–4231.
(18) Friesen, J. B.; Pauli, G. F. *J. Agric. Food Chem.* **2008**, *56*, 19–28.
(19) Friesen, J. B.; Pauli, G. F. *J. Chromatogr., A* **2007**, *1151*, 51–59.
(20) Pauli, G. F.; Pro, S. M.; Friesen, J. B. *J. Nat. Prod.* **2008**, *71*, 1489–1508.
(21) Inui, T.; Wang, Y.; Pro, S.; Cho, S.; Smith, D. C.; Franzblau, S. G.; Pauli, G. F. In *Structural Characterization of Anti-TB Active Principles from the Ethnobotanical Oplopanax horridus*; 48th Annual Meeting of the American Society of Pharmacognosy, Portland, ME, 2007; Ireland, C., Ed.; pp , P−134S.
(22) Abraham, W. R. *World J. Microbiol. Biotechnol.* **1993**, *9*, 319–322.
(23) Abraham, W. R. Braunschweig, Germany. Unpublished work, 2007.
(24) Nitz, S.; Spraul, M. H.; Drawert, F. *J. Agric. Food Chem.* **1990**, *38*, 1445–1447.
(25) Hsieh, T. J.; Lu, L. H.; Su, C. C. *Biophys. Chem.* **2005**, *114*, 13–20.
(26) Iida, T.; Nakano, M.; Ito, K. *Phytochemistry* **1982**, *21*, 673–675.
(27) Pelter, A.; Ward, R. S.; Venkata Rao, E.; Sastry, K. V. *Tetrahedron* **1976**, *32*, 2783–2788.
(28) Becker, E. D.; Beroza, M. *Tetrahedron Lett.* **1962**, 157–163.
(29) Tuntiwachwuttikul, P.; Phansa, P.; Pootaeng-on, Y.; Taylor, W. C. *Chem. Pharm. Bull.* **2006**, *54*, 149–151.
(30) Bernart, M. W.; Cardellina, J. H., 2nd; Balaschak, M. S.; Alexander, M. R.; Shoemaker, R. H.; Boyd, M. R. *J. Nat. Prod.* **1996**, *59*, 748–753.
(31) Inui, T. Phytochemical and biochemometric evaluation of the Alaskan anti-TB ethnobotanical: *Oplopanax horridus*. Ph.D. Thesis, University of Illinois at Chicago, Chicago, IL, 2008, p 193.
(32) Collins, L. A.; Franzblau, S. G. *Antimicrob. Agents Chemother.* **1997**, *41*, 1004–1009.
(33) Franzblau, S. G.; Witzig, R. S.; McLaughlin, J. C.; Torres, P.; Madico, G.; Hernandez, A.; Degnan, M. T.; Cook, M. B.; Quenzer, V. K.; Ferguson, R. M.; Gilman, R. H. *J. Clin. Microbiol.* **1998**, *36*, 362–366.
(34) Cantrell, C. L.; Lu, T.; Fronczek, F. R.; Fischer, N. H.; Adams, L. B.; Franzblau, S. G. *J. Nat. Prod.* **1996**, *59*, 1131–1136.

NP900674D